Tikrit Journal
for
Dental Sciences
https://tjo-ds.com

# Mechanical Properties Evaluation of Magnesium-Based Alloy Used for Dental Implant Synthesis

Safwan Abid Al-Hameed Suliman [1]
Hikmat Jameel Aljudy [2]

[1] Department of Prosthodontics, College of Dentistry, Tikrit University-Iraq.

[2] Department of Prosthodontics, College of Dentistry, University of Baghdad. Baghdad-Iraq.

**Article Info:**
**-Article History:**
**-Received:** 15/2/2021
**-Accepted:** 28/3/2021
**-Available Online:**
**J**un, 2022

**Keywords:**
Dental alloy, Dental implant Prosthodontics, Mechanical properties.

**Corresponding Author:**
**Name:** Safwan Abid Al-Hameed Suliman
**E-mail:**
safwanalsabaawi@tu.edu.iq
**Tel:**
**Affiliation:**
Ph. D. student, Department of Prosthodontics, College of Dentistry, Tikrit University-Iraq.

**Abstract**

**Background:** Mg as well as its alloys are differing from other biomaterials through providing compatible physical and mechanical characteristics to the human bones. Also, their elastic modulus and densities were somewhat close to one another and thus removing elastic mismatches between the bone and implants. Furthermore, the Mg present naturally in bone structure, and it is essential metal for metabolism. Some mechanical properties (Hardness, diametral tensile) and corrosion resistance of enforced Mg by Strontium and alloyed with another biocompatible elements (Zn, Mn) were examined. **Materials and methods:** 135 samples were prepared for microhardness, diametral tensile, and corrosion test, divided to two groups 1st one pure Mg as a control group, 2nd group Mg alloy with different concentration of alloying elements to select the optimum ratio for alloying elements which consist of Zinc, Manganese, and Strontium). **Result:** Alloying of Mg with Zn, Mn and Sr, shows improvement in mechanical properties but dropping in corrosion resistance when compared with pure Mg. **Conclusions:** Alloying of pure Mg by ternary Zn, Mn and Sr have a valuable improvement in mechanical micro hardness and diametral tensile properties, but increases corrosion rate in comparison with pure Mg due to the effect of galvanic corrosion.

## Introduction:

The fundamental aim behind the development of an alloy is improving the mechanical characteristics, resistance to corrosions and reducing the costs of the production [(1)]. The main elements which are utilized for the alloying of magnesium are Ca, Cu, Fe, Al, Mn, Ni, Sr, Li, Zn, Zr, RE, and Y [(2-5)]. However, the characteristics of the alloy are dependent as well on the inter-metallic complex and the micro-structural effects which have been based upon the route of the processing. The non-toxic alloying elements have to be utilized for the

humans. Some elements like the Mn, Zn, and Ca are significant trace elements for the human life and RE elements which exhibit anti-carcinogenic characteristics have to be the primary option for incorporating to the alloy [6].

## Materials and Methods:

**Specimen Design**

Cylindrical specimens were prepared with (15mm) diameter and (15mm) height for compression, and corrosion test; other specimens were prepared with (10mm) diameter and (10mm) height for Vickers hardness test.

**Mold design**

The mold was made from steel tool material, it was consisting from four parts; die, base, punch guide and punches.

**Sample grouping for invitro testing**

One hundred thirty-five specimens were prepared and subdivided into nine groups each group contain fifteen samples, according to the different percentage of alloying elements, as shown in table 1:

Each group compacted under 500 MPa pressure at 25ºC for two minutes prior to releasing the load and sintered at a temperature of 400ºC for 1 hour soaking time within continual argon flow. Each group subdivided into three subgroups each subgroup composed of five specimens for compression, microhardness hardness test, and corrosion test, as shown in figure 1.

**Mixing and Ball Milling**:

A sensitive accurate electronic balance with 0.1 mg accuracy was used to weight Mg powder that was dried at 120 °C before mixing. Sr, Mn, Zn and Mg powder have been utilized as raw materials. Also, the Mg is considered as the base and matrix in composite material, whereas Sr, Mn and Zn were utilized as elements for alloying. The mixing was conducted in planetary ball mill. The starting materials Mg-Sr then Zn and Mn were added followed by addition of an organic material that is considered as 3% n-heptane solution has been added as process control agent or surfactant in the mixture for preventing agglomeration throughout the mechanical alloying procedure, all the materials were placed in stainless- steel mill vial. In addition, the stainless-steel milling balls with fixed 5:1 ball/powder weight ratio (BPR) are put with powders, while the argon gas is applied in vial for preventing powders from contamination or oxidation. Also, the rotational speed of the milling is 300rpm for 2hours, milling duration and intervals of 30mins milling and 30mins rest has been fixed, the short milling time with low ball/powder weight ratio is set for avoiding the generation of extreme heat at high speed of the milling [7].

**Compaction**

Cold compaction was performed in uniaxial way by hydraulic press supplied by digital gage, under pressure of 650MPa and holding time of 2mins at 25°C before releasing the load to overcome any spring-back effect. Two sets of pressing molds were used first for the production of 15 mm diameter cylindrical samples and the second for 10 mm diameter cylinder like shape samples.

**Sintering:**

The compacted composites are sintered in the sintering system for 1 hour soaking time, at a temperature of 400°C under continuous argon flow. For the purpose of ensuring the samples were heated (homogenously), heating rate (5°C/min) is utilized for cooling and heating cycles [7].

**Microhardness test**

Vickers microhardness test was done according to ASTM (E92-82) for specimens of each group, the cylindrical specimens were used in this test with diameter of samples was (10mm) and height (10mm) well finished and polished. This apparatus was used to measure hardness with 1000g load and holding time of 20 seconds dwell time to the surface of the specimen using a standard 136°. At least five measurements for each sample were measured in order to obtain the accurate average hardness number. Vickers diamond pyramid indenter combined with optical microscopy to measure the diagonal length of Vickers impression, diamond pyramid indenter should be away from margin about 2mm

and away from each other indentation about 2mm then mean of five reading would be used for each sample.

**Diametral tensile test**

It is indicated as the diametral compression test, such test might be utilized just for the materials showing elastic deformations primarily and no or little plastic deformations, while the vertical compressive force along the cylinder's side is producing a tensile stress which is considered to be perpendicular to vertical plane that pass through the disc center. Fracture happens along such vertical plane (dashed vertical line on cylinder). The load of 1000N and crosshead speed 1mm/min utilizing universal testing machine.

**Corrosion test**

The cylindrical samples with thickness of 15mm and diameter of 15 mm are utilized for electrochemical tests. The samples are attached to the Cu wire and mounted in epoxy resin with a 10 $mm^2$ exposed area as working electrode.

Prior to electrochemical test, the mounted sample is effectively polished by 1500, 2000 after that 3000-grit silicon carbide paper with the cooling water flow and after that polished with diamond suspension of 1.0 μm, after that adequately degreased with ethanol and acetone and rinsed by distilled water, lastly; the samples dried by warm air stream. In addition, the open circuit potential (OCP) as well as the curves of the potentio-dynamic polarization for the samples which are soaked in simulated body fluid (SBF) [8]. Furthermore, Electrochemical system supplied via 3 electrode cell system with the saturated calomel electrode (SCE) as the reference electrode, platinum electrode (15x15 $mm^2$) as counter electrode, also the sample which has been mounted in the epoxy resin as working electrode. The scan rate is 1Mv/sec. for thirty minutes for each of the sample. All experiments are conducted at temperature 37°C which regulated by thermostat. Corrosion density current ($I_{corr}$) measured to estimate the corrosion rate which directly proportion to each other.

## Results and Discussions:

**Microhardness test:**

The microhardness (Vickers hardness test) of consolidated specimens was measured according to ASTM (E9-89a) for each group of specimens by using digital microhardness Vickers tester apparatus. The specimens of group IX showed the higher microhardness with mean value (50.41Kg/$mm^2$) and the specimens of Pure Mg showed the lower microhardness with mean value (40.3Kg/$mm^2$) as shown in table 2:

**Diametral tensile test**

The diametral tensile test of consolidated specimens were measured according to **ASTM E9-89a** standard method for compression testing of metallic materials at room temperature, then the average was calculated for five readings. The data gained from Instron universal testing machine were summarized by table 3.

The diametral tensile test results of present study showed that the specimens of **Group IX** had the highest value of diametral tensile force.

**Corrosion test**

The corrosion test of consolidated specimens was carried out according to ASTM standards F2129, G61, the sample was immersed in SBF at 37°C temperature, by using Potentiostat, the average was calculated for five readings.

The corrosion test results of present study showed that the specimens of **Group IX** had the lower value of $\boldsymbol{I_{corr}}$ comparing to other concentration, while **Group I** have the lowest value. The data gained from corrosion test were summarized by table 4:

The results of this study revealed that the group (IX) which composed of Mg 94%, Zn 4%, Mn 1% and Sr 1% have a higher hardness in microhardness test, higher value in diametral tensile test and better corrosion resistance in SBF at 37°C when compared with other groups (II, III, IV, V, VI, VII, and VIII) that include different concentration of alloying element. According to the previous results of three tests found that the optimum concentration of raw materials was **Group IX**.

## Discussion

All titanium-based alloy are regarded as bioinert materials but they do not allow bone formation on their surface leading to weak bonding between the implants and bone [9]. Mg and its alloys differ from other biomaterials by presenting compatible mechanical and physical properties to human bone. Their densities and elastic modulus are fairly close to each other which remove elastic mismatches between implants and the bone [10,11]. Moreover, Mg is naturally present in bone composition, and it is one of the required metals for the metabolism [12]. However, the fundamental problem of Mg-based implant is their low corrosion resistance resulting undesirable fast and unexpected degradation within a living system. Implant material is desired to have very similar mechanical properties with the bone. However, in the current practice, most of the metals used in biomedical applications exhibit significantly higher mechanical properties than the bone. This causes well-known phenomenon of stress shielding, which are results of bone-matter decomposition and loss of its strength. Stress shielding occurs when the implant carries higher proportion of the applied load, so the adjacent bone is exposed to increased load and loses its density in response [13].

**Microhardness:**

Microhardness of Mg-based compacts increases as alloying elements are added into the Mg-based composite. The microhardness of Mg-Zn-Mn-Sr compacts with ratio (94%,4%,1% and 1%wt) respectively shows the highest value among the alloyed Mg-based compacts and pure Mg. Alloying elements usually elevate the strength of the alloy either by *grain refinement* (grain boundary strengthening or Hall–Petch strengthening) which improves both strength and ductility [14]. Mechanical interlocking of powder particles occurs when the surface of the powder particles become enmeshed. During plastic deformation the contact areas between adjacent particles grow and interparticle bonding can occur. Generally, as the compaction pressure increases, so does the degree of interlocking, although other factors, such as the type of powder and particle shape are also important [15]. Solid bridges or cold welding occurs when the interparticle loads become sufficient to break down the surface oxide layers and cause metal-metal contact [16], or this may due to *lattice distortion effect* where multi-element lattice is highly distorted because all the atoms are solute atoms and their atomic sizes are all different from one another [17].

The addition of **Zn** to Mg based alloy with proportion of 4%wt would increase the microhardness significantly, this results agree with Gao et al.in 2008 and Hänzi et al. in 2009 they found that the addition of Zinc up to 3 wt.% has a beneficial effect on strength with the formation of Mg–Zn phase [18,19]. Zinc is known to be a good solid solution and precipitation strengthening agent in Mg alloys [20,21]. It is one of the most commonly used alloying elements in Mg [22].

The addition of **Mn** to Mg based alloy with proportion of 1%wt would increase the microhardness significantly, also Mn is added to many commercial alloys to reduce the harmful effects of impurities [23]**.** With the addition of alloying elements, the agglomeration of the particle is significantly reduced specially with the addition of Mn element. Much finer particle size is obtained with addition of Mn than with just the addition of Zn in the Mg. Better refinement of particle size occurred with the addition of Zn and Mn in combination in Mg-based composite. The addition of crystalline material such as Zn and Mn in the Mg-based composite seems to reduce the particle size as well as increase the homogeneity in size of the powder. This may be due to the resultant harder phase formation on ternary addition. The harder particles break easily to finer sizes as compared to ductile phases [7].

The addition of **Sr** to Mg based alloy with proportion of 1%wt significantly improve microhardness of Mg alloys, this result would agree with Zeng et al. in 2006 and Fan et al. in 2007**,** they reported that small doses of Sr can effectively refine the grain size of the AZ31 magnesium alloy [24,25],

also agree with Lai et al in 2018 found that the average grain size of the Mg-Zn-Sr alloys was reduced significantly as the amount of added Sr increased from 0.1 to 0.5 wt.%.which affect the mechanical properties of Mg alloy [26]. While Cu et al. in 2012 found the Sr content when increases from 3 to 4 wt.%, the grain size is not obviously refined while the formation of $Mg_{17}Sr_2$ intermetallic phases increases, which would be a crack source with a harmful effect on the ductility and strength of Mg alloys [27]. The result will disagree with Borkar et al.in 2012 they found that the addition of more than 0.7 wt.% Sr leads to recrystallization which would decrease the mechanical properties of Mg-based alloys [28]. Sr is commonly added to Mg as a grain refiner due to its tendency to form compounds that segregate to grain boundaries [24]. However, combinations of Zn and Sr in Mg alloys remain largely unstudied. Additionally, studies on the microstructural features of Mg–Zn–Sr alloys are lacking in the literature and the most current calculations of phase equilibria that can be found on this system are based on extrapolations from binary Mg–Zn, Mg–Sr, and Sr–Zn behaviors [29].

**Diametral tensile (Diametral Compression Test):**

Diametral tensile of Mg-based composites increases as alloying elements are added into the Mg-based compacts. The Diametral tensile of Mg-Zn-Mn-Sr compacts with ratio (94%,4%,1% and 1%wt) respectively shows the highest mean value among the alloyed Mg-based composites and pure Mg. The addition of ternary alloying elements in Mg-based composite shows the highest ultimate compressive strength this is because the dispersion of both Zn, Mn, and Sr as alloying elements in the Mg matrix give solid solution strengthening effect as on deformation dislocation movement is obstructed by the stressed matrix increasing the compressive strength and diametral tensile strength of the composites [30]**.** It can also be inferred that the compressive strength is directly proportional to the hardness as increasing the hardness may increase the compressive strength. In binary alloying of Mg-based composite, the addition of Zn shows better strengthening than the addition of Mn since Zn is considered next to Al in strengthening effectiveness as an alloying element in Mg. Elongation of quaternary alloys increased with increases in Zn content up to 4 wt.%. The enhancement of ultimate tensile strength is due to the grain refining and solution strength effects and second phase strengthening [31]. The results agree with Zhang et al. in 2011 they found that Zn is an important alloying element with a relatively high solubility in Mg, Zn content that is up to 4 wt.% significantly increases the ultimate tensile strength and elongation of Mg–Zn alloys, but any higher percentage of Zn would lead to the reduction of both properties and decrease the corrosion resistance of the alloy, but it was shown that amorphous Mg–Zn-based alloys containing about 5.0 wt.% of Zn had excellent strength, high corrosion resistance, low hydrogen evolution rate, and good biocompatibility in animals; therefore, these are promising candidates for biodegradable bone implants [32]. Due to Mg-Zn intermetallic compound formation and refining the grain size, addition of Zn to the Mg matrix improves strength [33,34]. Zn can play dual roles in both solid solution and precipitation strengthening [35,36]**.** Zn also can increase age hardening response as it produces intermetallic compounds and refine the grain size [35,37]. The microstructure of binary as-cast Mg-Zn alloy consists of primary α-Mg matrix and MgZn intermetallic phase distributing along the grain boundary [38,39]. Grain refinement can also remarkably increase the grain boundaries densities and inhibit the dislocation movement, thus delaying the formation and expansion of the micro-cracks [40]. Therefore, the finer grains were favorable for the occurrence of grain boundary glide, which improved the ductility [41]. The addition of Zn to Mg alloys resulted in an increase in both the yield and ultimate tensile strengths of the material due to Zn's favorable solid solution and precipitation response [42].

Mn a widely used alloying element in Mg alloys to improve the tensile strength and weldability [43]. The addition of Mn was

found to have remarkable effect of finer grain size in the extruded condition. The enhancements of tensile properties (yield stress, tensile strength, and total elongation) with respect to observed grain refinement [44]. The grain size decreased with increasing Mn content and attained a constant grain size at the Mn contents higher than 0.4 wt.%, where the intermetallic particles were precipitated. The tensile strength and hardness increased with increasing Mn content and attained a constant value at the Mn contents higher than 0.4 wt.%, which was consistent with the grain size variation. The Mn contents provide a good balance of mechanical properties and fatigue strength in magnesium alloys [45]**.** The improvement of mechanical properties of Mg alloys can be attributed to the combined effects of refined microstructure, weakened basal texture and high density of nanoscale Mn precipitates locating among the matrix and along the grain boundary, dislocations and faults [46]. While undissolved phases distributed along the recrystallized grain boundaries effectively refined the microstructure of Mg alloy during extrusion process, leading to a marked increase in strength and elongation [47].

The diametral tensile value of the based alloy was increased by adding Sr up to 1 wt.% which agree with Şevik and Kurnaz [48] they found that the addition of this critical weight percentage Sr ratio, the tensile strength starts to drop with increasing Sr addition more than1%. The typical metallographic microstructure of the Mg-Sr binary alloys mainly consists of α-Mg grains, and the second phase $Mg_{17}Sr_2$ precipitated along the grain boundaries [49]. Sr has the effect of grain refinement; the refined eutectics lead to strong dispersion strengthening. However more than 3% Sr addition will deteriorate the mechanical properties of Mg-Sr alloy due to less formation of intermetallic with weaker dispersion strengthening. Addition of Sr to Mg alloy showed the best combination of strength and ductility [50,51]. Addition of Sr inducing microstructural changes that relate to grain size, stringer formation, twinning suppression and dislocation activity, all of which cause distinct changes in the bulk mechanical behavior investigated by compression both parallel and perpendicular to the c-axis [52]. The grain refinement promoted the strength and ductility, while the excessive secondary phases resulted in the degradation of the mechanical performance. The combined actions of finer grain size and smaller secondary phases content contributed to the optimal mechanical performance of the Mg alloy [53]**.**

**Corrosion test:**

A dense distribution of precipitates and reduction of grain size would improve the mechanical properties but accelerate the degradation rates at the same time [54]. Micro-pores would reduce the corrosion resistance of Mg alloys owing to an auto-catalytic corrosion cell formed by corrosion products stuck in pores which would lead to severe localized corrosion, and high porosity density results in a greater exposed area [50,55]. The Mg-based compact with addition of Zn, Mn and Sr as alloying elements with ratio (94%,4%,1% and 1%wt) respectively showed the lowest corrosion rate among the other Mg-based compact. This result show similar trends as reported by Xu et al. in 2008 that alloying elements in Mg alloy can reduce the weight loss since more elements can react and form a protective layer on the surface of the composite **[56]**. Also; Hussain Z. in 2017 observed that the addition of alloying elements into Mg-based composite can increase the corrosion resistance [57]. However, once the content of Zn exceeded 1 and up to 2 wt.%, other species secondary phases containing Zn, accelerated the dissolution rate of the Mg matrix. The micro-galvanic corrosion occurred at the interface area between the Mg matrix and Zn secondary phase, leading to the formation of micro cracks between them. As the corrosion process prolonged, Mg matrix around the Zn dissolved unceasingly, resulting in the extension of the cracks **[41]**. The Zn effect on the increase in the $H_2$ evolution rate was more pronounced than the reduction in the $I_{passive}$, therefore the overall corrosion rate at open circuit condition were increased by alloying Zn **[58]**. The

binary alloying elements in Mg-based composites show that element addition of Mn causes less weight loss than composite containing Zn. Therefore, it seems that Mn is more effective to enhance corrosion resistance of Mg-based composite since Mn have been improving the saltwater resistance of magnesium alloy by removing iron and other heavy-metal elements while Zn has tendency to fast corroded rather than Mn [59]. The main role of Mn was to reduce the content of impurities (Fe, Ni), so as to reduce the corrosion effect of impurities. During the degradation process, the pure Mg had a lower Volta potential than the Mg alloy matrix, which acted as the anodic and consequently protected the Mg matrix from pit corrosion, exhibiting the uniform degradation morphology. Inversely, the Volta potentials of the other Zn-containing phases/inter metallics were higher than the matrix, which can act as the cathode and accelerate the degradation rate of Mg matrix.[41]. The mechanism of the action of manganese on the corrosion resistance of magnesium alloys containing an iron admixture as an inevitable impurity (in a number of hundredths of wt.%) is commonly explained by the following factors:

**a.** manganese in magnesium alloys with aluminum suppresses the formation of aluminum phases with iron, and the formed-Mn phase has a more negative potential and a higher hydrogen super potential.

**b**. manganese forms a number of solid solutions with iron; they hinder the depolarization of the microscopic cathodes, i.e., impurities, which lowers the corrosion rate on the whole **[60]**. Both the electrochemical and the hydrogen evolution tests indicated that Mn addition gradually improved the corrosion resistance of the Mg alloys in NaCl solution. [61]. The Electrochemical impedance spectroscopy (EIS) analysis indicate that the addition of Mn improves the corrosion resistance of Mg alloy because Mn purifies the matrix by removing harmful impurities. Intergranular corrosion and galvanic corrosion increases with the continuous addition of Mn [62]. While Sr would impair the corrosion resistance due to the redundant insoluble Sr which forms potential difference with magnesium **[63]**. In addition, the reduction of grain size increases the surface tension and interaction with adjacent grains, so that lattice deformation appears and the tensile strength and plasticity of Mg alloys are elevated [64]. Sr additions contributed to different corrosion resistance and dissolution rate of the alloys. Alloys with better corrosion resistance dissolved slower at the initial time and were more inclined to adsorb the $Mg^{2+}$ and $OH^-$ ions in the SBF forming the Mg $(OH)_2$ layers. The corrosion inhibiting effect is achieved by the coverage effect of the corrosion product layers. A denser and thicker hydroxide protective film reduced the dissolution rate of the alloy and thus reduced the production rate of $OH^-$ ions. Although the corrosion product layers played a certain protective role, the micro-pores in the hydroxide film left by the dissolution of Sr $(OH)_2$ made it easily for the chloride ions in the SBF to pass through the surface protective layer and react directly with the inner Mg $(OH)_2$ to transform the hydroxides into soluble metallic $Mg^{2+}$ ions and $OH^-$. The chloride ions accelerated the corrosion around the micro-pores and the deposition of the corrosion products. This gave rise to localized corrosion. Continuously released $OH^-$ ions resulted in a higher pH value near the surface, accelerating the nucleation and growth of phosphates and their eventual coverage on the Mg $(OH)_2$ layer. As the corrosion reaction proceeded further until the SBF contacted the second phase $Mg_{17}Sr_2$, micro-galvanic corrosion occurred between the Mg matrix and the secondary phases. The anodic reaction transformed Mg into $Mg^{2+}$ ions, while the cathodic reaction transformed $H_2O$ into $OH^-$. Grain refinement improve the corrosion resistance by reducing the concentration of impurities and forming a denser corrosion product layer, while the secondary phases accelerated the corrosion process by forming micro galvanic couples with the Mg matrix. The Sr content increase the grain refinement effect which play a dominant role in the

corrosion behavior. Once the added Sr content was equal to or greater than 0.3 wt.%, the dominant influence factor became the secondary phases [53]. Gu et al. in 2012 have studied the in vitro and in vivo performance of the as-rolled Mg–Sr alloys with Sr addition ranging from 1 to 4 wt% and proved that the as-rolled Mg–2Sr alloy presented finer microstructure, highest ultimate tensile strength, slower degradation rate and superior osteogenic properties during 4 weeks implantation among other alloys [27].

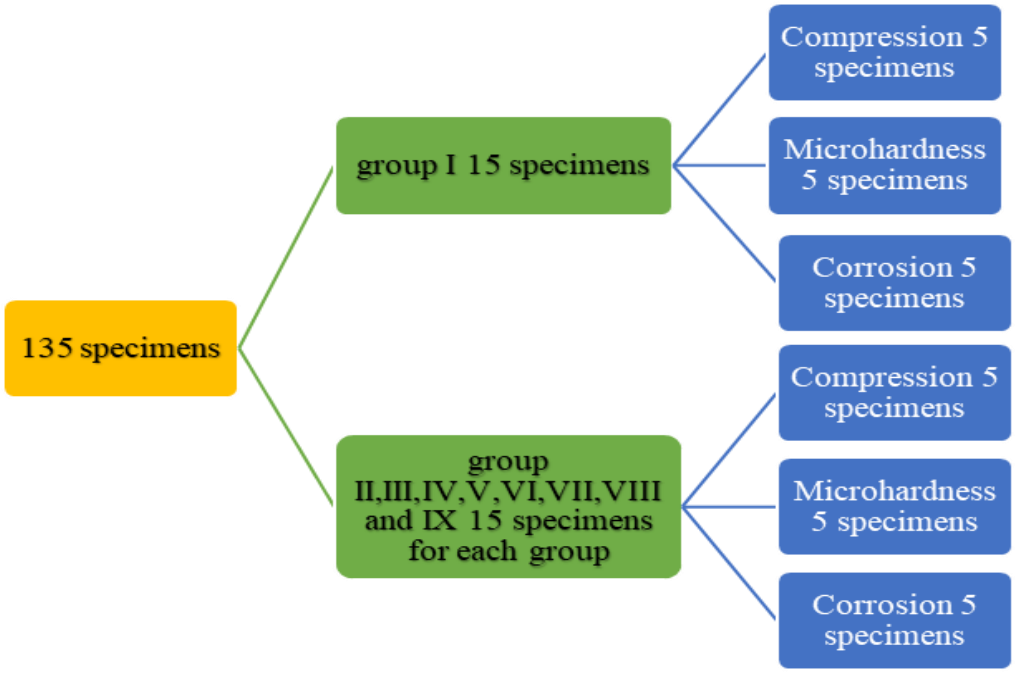


Figure 1: Sample grouping of invitro pilot study.

**Table 1: Percentage of alloying elements used in pilot study**

| Groups | Mg wt% | Zn wt% | Mn wt% | Sr wt% |
|---|---|---|---|---|
| Pure Mg (control) Group I | 99.95 % | | | |
| Group II | 97% | 2% | 0.5 | 0.5 |
| Group III | 95% | 4% | 0.5 | 0.5 |
| Group IV | 96.5% | 2% | 1 | 0.5 |
| Group V | 94.5% | 4% | 1 | 0.5 |
| Group VI | 96.5% | 2% | 0.5 | 1 |
| Group VII | 94.5% | 4% | 0.5 | 1 |
| Group VIII | 96% | 2% | 1 | 1 |
| Group IX | 94% | 4% | 1 | 1 |

**Table 2: Mean values of microhardness test for nine groups of specimens**

| $Kg/mm^2$ | Sample 1 | Sample 2 | Sample 3 | Sample 4 | Sample 5 | Mean |
|---|---|---|---|---|---|---|
| Group I Pure Mg | 42.5 | 38.6 | 39 | 42 | 40 | 40.4 |
| Group II | 45.6 | 43.4 | 46 | 44.5 | 44.8 | **44.86** |
| Group III | 48.9 | 47.4 | 49.6 | 47.3 | 48.6 | **48.36** |
| Group IV | 44.7 | 43.4 | 42.3 | 45.8 | 46.5 | **44.54** |
| Group V | 48 | 45.7 | 46.8 | 49 | 48.8 | **47.66** |
| Group VI | 43 | 42 | 43.9 | 44.8 | 41.3 | **43.6** |
| Group VII | 48 | 47.2 | 48.7 | 49.9 | 47.7 | **48.4** |
| Group VIII | 49.2 | 46.8 | 47.3 | 47.7 | 49.1 | **47.98** |
| Group IX | 52 | 50 | 51 | 50 | 49.7 | **50.54** |

**Table 3: Mean values of diametral tensile test for eight groups of specimens**

| $\sigma$ $N/mm^2$ | Sample 1 | Sample 2 | Sample 3 | Sample 4 | Sample 5 | Mean |
|---|---|---|---|---|---|---|
| Group I Pure Mg | 10.5 | 12.1 | 10.3 | 9.8 | 11.3 | 10.8 |
| Group II | 13.2 | 13.5 | 12.8 | 13.6 | 12.9 | 13.2 |
| Group III | 13.9 | 14.6 | 13.3 | 14.1 | 13.7 | 13.92 |
| Group IV | 14.3 | 13.7 | 13.5 | 13.6 | 14.2 | 13.86 |
| Group V | 13.1 | 13.5 | 13.7 | 13.4 | 13.6 | 13.46 |
| Group VI | 13.4 | 13.4 | 13.5 | 13.7 | 13.2 | 13.4 |
| Group VII | 13.4 | 13.8 | 13.7 | 13.6 | 13.3 | 13.56 |
| Group VIII | 13.6 | 13.2 | 13.1 | 12.9 | 13.4 | 13.2 |
| Group IX | 13.7 | 14.3 | 13.9 | 13.7 | 14.5 | 14.02 |

**Table 4: Mean values of corrosion test for eight groups of specimens**

| $I_{corr}$ µA/cm$^2$ | Sample 1 | Sample 2 | Sample 3 | Sample 4 | Sample 5 | Mean |
|---|---|---|---|---|---|---|
| Group I Pure Mg | 126 | 124 | 126 | 127 | 123 | 125.2 |
| Group II | 210.1 | 236.98 | 227.6 | 223.5 | 225.4 | 224.71 |
| Group III | 226.62 | 229.72 | 227.3 | 226.65 | 227.34 | 227.52 |
| Group IV | 227.74 | 225.34 | 224.76 | 224.82 | 225.63 | 225.65 |
| Group V | 227.57 | 232.88 | 228.55 | 227.76 | 231.63 | 229.6 |
| Group VI | 207.46 | 216.72 | 224.32 | 215.58 | 217.54 | 216.33 |
| Group VII | 183.66 | 181.6 | 179.85 | 182.5 | 180.7 | 181.7 |
| Group VIII | 171.93 | 179.52 | 176.84 | 173.84 | 177.72 | 175.9 |
| Group IX | 163.05 | 176.77 | 169.47 | 170.62 | 168.92 | 169.76 |

# References


1. WITTE, F., HORT, N., VOGT, C., COHEN, S., KAINER, K. U., WILLUMEIT, R. & FEYERABEND, F. 2008. Degradable biomaterials based on magnesium corrosion. Current opinion in solid state and materials science, 12, 63-72.

2. WITTE, F., KAESE, V., HAFERKAMP, H., SWITZER, E., MEYER-LINDENBERG, A., WIRTH, C. & WINDHAGEN, H.2005. In vivo corrosion of four magnesium alloys and the associated bone response. Biomaterials, 26, 3557-3563.

3. WITTE, F., FISCHER, J., NELLESEN, J., CROSTACK, H.-A., KAESE, V., PISCH, A. BECKMANN, F. & WINDHAGEN, H. 2006. In vitro and in vivo corrosion measurements of magnesium alloys. Biomaterials, 27, 1013-1018.

4. MÜLLER, W. D., NASCIMENTO, M. L., ZEDDIES, M., CÓRSICO, M., GASSA, L. M. & MELE, M. A. F. L. D. 2007. Magnesium and its alloys as degradable biomaterials: corrosion studies using potentiodynamic and EIS electrochemical techniques. Materials Research, 10, 5-10.

5. ZHANG, G., HUANG, J., YANG, K., ZHANG, B. & AI, H. 2007. Experimental study of in vivo implantation of a magnesium alloy at early stage. Jinshu Xuebao/Acta Metallurgica Sinica, 43, 1186-1190.

6. POINERN, G. E. J., BRUNDAVANAM, S. & FAWCETT, D. 2012. Biomedical magnesium alloys: a review of material properties, surface modifications and potential as a biodegradable orthopaedic implant. American Journal of Biomedical Engineering, 2, 218-240.

7. ZUHAILAWATI, H., N, M. & BK, D. 2017. Effect of Alloying Elements on Properties of Biodegradable Magnesium Composite for Implant Application. Journal of Powder Metallurgy & Mining, 06.

8. LI, N. & ZHENG, Y. 2013. Novel Magnesium Alloys Developed for Biomedical Application: A Review. Journal of Materials Science & Technology, 29, 489-502.

9. RATH, P. C., BESRA, L., SINGH, B. P. & BHATTACHARJEE, S. 2012. Titania/hydroxyapatite bi-layer coating on Ti metal by electrophoretic deposition: Characterization and corrosion studies. Ceramics International, 38, 3209-3216.

10. CHEN,Y.,XU., Z.,SMITH, C., &SANKAR, J.,2014. Recent advances on the development of magnesium alloys for biodegradable implants. Acta

biomaterialia, 10, 4561-4573.

**11.** DOROZHKIN, S. V. 2014. Calcium orthophosphate coatings on magnesium and its biodegradable alloys. Acta Biomaterialia, 10, 2919-2934.

**12.** SARIS, N.-E. L., MERVAALA, E., KARPPANEN, H., KHAWAJA, J. A. & LEWENSTAM , A. 2000. Magnesium: an update on physiological, clinical and analytical aspects. Clinica chimica acta, 294, 1-26.

**13.** CHIU, K., WONG, M., CHENG, F. & MAN, H. 2007. Characterization and corrosion studies of fluoride conversion coating on degradable Mg implants. Surface and Coatings Technology, 202, 590-598.

**14.** STAIGER, M. P., PIETAK, A. M., HUADMAI, J. & DIAS, G. 2006. Magnesium and its alloys as orthopedic biomaterials: a review. Biomaterials, 27, 1728-1734.

**15.** PAMUKKALE, Ü. N. İ. V. İ., M Ü HEND, İ. & KFAK, Ü. L. İ. 1996. MECHANICS OF DYNAMIC POWDER COMPACTION PROCESS. Journal of Engineering Sciences, 2, 129-134.

**16.** BOWDEN, F. & TABOR, D. 1967. Friction and Lubrication, Methuen & Co. Ltd. London.

**17.** JIEN-WEI, Y. 2006. Recent progress in high entropy alloys. Ann. Chim. Sci. Mat, 31, 633-648.

**18.** GAO, J.-C., SHA, W., QIAO, L.-Y. & YONG, W. 2008. Corrosion behavior of Mg and Mg- Zn alloys in simulated body fluid. Transactions of Nonferrous Metals Society of China, 18, 588-592.

**19.** HÄNZI, A. C., GUNDE, P., SCHINHAMMER, M. & UGGOWITZER, P. J. 2009. On the biodegradation performance of an Mg–Y– RE alloy with various surface conditions in simulated body fluid. Acta biomaterial, 5, 162-171.

**20.** CLARK ,J. 1965. Transmission electron microscopy study of age hardening in a Mg-5 wt.% Zn alloy. Acta Metallurgica, 13, 1281-1289.

**21.** BUHA, J. 2008. Reduced temperature (22–100° C) ageing of an Mg–Zn alloy. Materials Science and Engineering: A, 492, 11-19.

**22.** AVEDESIAN, M. M. & BAKER, H. 1999a. ASM specialty handbook: magnesium and magnesium alloys. ASM international, 274.

**23.** SONG, G. L. & ATRENS, A. 1999. Corrosion mechanisms of magnesium alloys. Advanced engineering materials, 1, 11-33.

**24.** ZENG, X., WANG, Y., DING, W., LUO, A. A. & SACHDEV, A. K. 2006. Effect of strontium on the microstructure, mechanical properties, and fracture behavior of AZ31 magnesium alloy. Metallurgical and Materials Transactions A, 37, 1333-1341.

**25.** FAN, Y., WU, G. H. & ZHAI, C. Q. Effect of strontium on mechanical properties and corrosion resistance of AZ91D. Materials science forum, 2007. Trans Tech Publ, 567-570.

**26.** LAI, H., LI, J., LI, J., ZHANG, Y. & XU, Y. 2018b. Effects of Sr on the microstructure,
mechanical properties and corrosion behavior of Mg-2Zn-xSr alloys. Journal of Materials Science: Materials in Medicine, 29, 87.

**27.** GU, X., XIE, X., LI, N., ZHENG, Y. & QIN, L. 2012. In vitro and in vivo studies on a Mg–Sr binary alloy system developed as a new kind of biodegradable metal. Acta biomaterialia, 8, 2360-2374.

**28.** BORKAR, H., HOSEINI, M. & PEKGULERYUZ, M. 2012. Effect of strontium on flow behavior and texture evolution during the hot deformation of Mg–1 wt% Mn alloy. Materials Science and Engineering: A, 537, 49-57.

**29.** ALJARRAH, M., AGHAULOR, U. & MEDRAJ, M. 2007. Thermodynamic assessment of the Mg–Zn–Sr system. Intermetallic, 15, 93-97.

**30.** ZHANG, S., ZHANG, X., ZHAO, C., LI, J., SONG, Y., XIE, C., TAO, H., ZHANG, Y., HE, Y. & JIANG, Y. 2010. Research on an Mg–Zn alloy as a degradable biomaterial. Acta biomaterial, 6, 626-640.

**31.** CAI, S., LEI, T., LI, N. & FENG, F. 2012. Effects of Zn on microstructure, mechanical properties and corrosion behavior of Mg– Zn alloys. Materials Science and Engineering: C, 32, 2570-2577.

**32.** ZHANG, B., WANG, Y. & GENG, L. 2011. Research on Mg-Zn-Ca alloy as degradable biomaterial. Biomaterials-Physics and Chemistry, 183-204.

**33.** GHOSH, P., MEZBAHUL-ISLAM, M. & MEDRAJ, M. 2012. Critical assessment and thermodynamic modeling of Mg–Zn, Mg–Sn, Sn–Zn and Mg–Sn–Zn systems. Calphad, 36. 28-43.

**34.** MEZBAHUL-ISLAM, M., MOSTAFA, A. O. & MEDRAJ, M. 2014. Essential magnesium alloys binary phase diagrams and their thermochemical data. Journal of Materials, 2014.

**35.** Li, N.& ZHENG, Y. 2013. Novel Magnesium Alloys Developed for Biomedical Application: A review. Journal of Materials Science &Technology, 29,489-502.

**36.** ROSALBINO, F., DE NEGRI, S., SCAVINO, G. & SACCONE, A. 2013. Microstructure and in vitro degradation performance of Mg– Zn–Mn alloys for

biomedical application. Journal of Biomedical Materials Research Part A, 101A, 704-711.

**37.** SU, Z., LIU, C. & WAN, Y. 2013. Microstructures and mechanical properties of high-performance Mg–4Y–2.4Nd–0.2Zn–0.4Zr alloy. Materials & Design, 45, 466-472.

**38.** KUBASEK, J., VOJTECH, D.& POSPISILOVA, I. 2012. Structural and corrosion characterization of biodegradable Mg-Zn alloy castings. Kovove Mater, 50, 415-424.

**39.** KUBÁSEK, J. & VOJTĚCH, D. 2013. Structural characteristics and corrosion behavior of biodegradable Mg–Zn, Mg–Zn–Gd alloys. Journal of Materials Science: Materials in Medicine, 24, 1615-1626.

**40.** WANG, J., JIANG, W., MA, Y., LI, Y. & HUANG, S. 2018. Substantial corrosion resistance improvement in heat-treated Mg–Gd–Zn alloys with a long period stacking ordered structure. Materials Chemistry and Physics, 203, 352-361.

**41.** WEI, L., LI, J., ZHANG, Y. & LAI, H. 2020. Effects of Zn content on microstructure, mechanical and degradation behaviors of Mg-xZn-0.2 Ca-0.1 Mn alloys. Materials Chemistry and Physics, 241, 122441.

**42.** BRAR, H. S., WONG, J. & MANUEL, M. V. 2012. Investigation of the mechanical and degradation properties of Mg–Sr and Mg– Zn–Sr alloys for use as potential biodegradable implant materials. Journal of the mechanical behavior of biomedical materials, 7, 87-95.

**43.** GU, X., ZHOU, W., ZHENG, Y., DONG, L., XI, Y. & CHAI, D. 2010. Microstructure, mechanical property, bio-corrosion and cytotoxicity evaluations of Mg/HA composites. Materials Science and Engineering: C, 30, 827-832.

**44.** RAZZAGHI, M., MIRZADEH, H. & EMAMY, M. 2019. Mechanical properties of Mg-Al- Mn magnesium alloys with low Al content in the as-cast and extruded conditions. Materials Research Express, 6, 106521.

**45.** KHAN, S. A., MIYASHITA, Y., MUTOH, Y. & SAJURI, Z. B. 2006. Influence of Mn content on mechanical properties and fatigue behavior of extruded Mg alloys. Materials Science and Engineering: A, 420, 315-321.

**46.** YU, Z., TANG, A., HE, J., GAO, Z., SHE, J., LIU, J. & PAN, F. 2018. Effect of high content of manganese on microstructure, texture and mechanical properties of magnesium alloy. Materials Characterization, 136, 310-317.

**47.** JUNG, J.-G ,.PARK, S. H., YU, H., KIM, Y. M., LEE, Y.-K. & YOU, B. S. 2014. Improved mechanical properties of Mg–7.6Al–0.4Zn alloy through aging prior to extrusion. Scripta Materialia, 93, 8-11.

**48.** ŞEVIK, H. & KURNAZ, S. C. 2014. The effect of strontium on the microstructure and mechanical properties of Mg–6Al–0.3 Mn–0.3 Ti–1Sn. Journal of Magnesium and Alloys, 2, 214-219.

**49.** AYDIN, D., BAYINDIR, Z. & PEKGULERYUZ,M. 2013. The effect of strontium (Sr) on the ignition temperature of magnesium (Mg): a look at the pre-ignition stage of Mg–6 wt% Sr. Journal of Materials Science, 48, 8117-8132.

**50.** GU, X., XIE, X., LI, N. ZHENG, Y.&QIN, L. 2012.In vitro & in vivo studies on Mg-Sr binary alloy system developed as a new kind of biodegradable metal. Actabiomaterialia,8,2360-2374.

**51.** XI, H., JIHUA, C., HONGGE, Y., BIN, S., GUANGHAO, Z. & CHONGMING, M. 2013. Effects of minor Sr addition on microstructure and mechanical properties of the as-cast Mg–4.5 Zn–4.5 Sn–2Al-based alloy system. Journal of alloys and compounds, 579, 39-44.

**52.** HAZELI, K., SADEGHI, A., PEKGULERYUZ, M. & KONTSOS, A. 2013. The effect of strontium in plasticity of magnesium alloys. Materials Science and Engineering: A, 578, 383-393.

**53.** LAI, H., LI, J., LI, J., ZHANG, Y. & XU, Y. 2018a. Effects of Sr on the microstructure, mechanical properties and corrosion behavior of Mg-2Zn-x Sr alloys. Journal of Materials Science: Materials in Medicine, 29, 1-14.

**54.** HAMU, G. B., ELIEZER, D. & WAGNER, L. 2009. The relation between severe plastic deformation microstructure and corrosion behavior of AZ31 magnesium alloy. Journal of alloys and compounds, 468, 222-229.

**55.** SONG, G., ATRENS, A. & DARGUSCH, M. 1998. Influence of microstructure on the corrosion of diecast AZ91D. Corrosion science, 41, 249-273.

**56.** XU, L., ZHANG, E., YIN, D., ZENG, S. & YANG, K. 2008. In vitro corrosion behaviour of Mg alloys in a phosphate buffered solution for bone implant application. Journal of Materials Science: Materials in Medicine, 19, 1.1025-017

**57.** HUSSAIN Z, M. I. N. DHINDAW BK 2017. Effect of Alloying Elements on Properties of Biodegradable Magnesium Composite for Implant Application. J Powder Metall Min 6: 179.

**58.** HA, H.-Y., KANG, J.-Y., YANG, J., YIM, C. D. & YOU, B. S. 2013. Limitations in the use of the potentiodynamic polarisation curves to investigate the effect of Zn on the corrosion behaviour of as-extruded Mg–Zn binary alloy. Corrosion science, 75, 426-433.

**59.** AVEDESIAN, M. M. & BAKER, H. 1999b. ASM specialty handbook:

magnesium and magnesium alloys, ASM international.

**60.** VOLKOVA, E. 2017. Effect of iron impurity on the phase composition, structure and properties of magnesium alloys containing manganese and aluminum. Metal Science and Heat Treatment, 59, 154-160.

**61.** YAO, S., LIU, S., ZENG, G., LI, X., LEI, T., LI, Y. & DU, Y. 2019. Effect of Manganese on Microstructure and Corrosion Behavior of the Mg-3Al Alloys. Metals, 9, 460.

**62.** ZHAO, T., HU, Y., HE, B., ZHANG, C., ZHENG, T. & PAN, F. 2019. Effect of manganese on microstructure and properties of Mg- 2Gd magnesium alloy. Materials Science and Engineering: A, 765, 138292.

**63.** LI, H., PENG, Q., LI, X., LI, K., HAN, Z. & FANG, D. 2014. Microstructures, mechanical and cytocompatibility of degradable Mg–Zn based orthopedic biomaterials. Materials & Design, 58, 43-51.

**64.** WANG, J., ZHANG, Y.-N., HUDON, P., JUNG, I.- H., CHARTRAND, P. & MEDRAJ, M. 2015. Experimental study of the crystal structure of the Mg15− xZnxSr3 ternary solid solution in the Mg–Zn–Sr system at 300 C. Materials & Design, 86, 305-312.